JGR Space Physics

RESEARCH ARTICLE
10.1029/2020JA028716

Key Points:

- The first observation of linearly polarized N^+ electromagnetic ion cyclotron wave is reported
- The observed wave activity suggests the presence of N^+ ions in the inner magnetosphere
- Possible generation mechanisms of N^+ EMIC wave are discussed

Supporting Information:

- Supporting Information S1
- Figure S1
- Figure S2

Correspondence to:
M. Fraz Bashir,
frazbashir@epss.ucla.edu

Citation:
Bashir, M. F., & Ilie, R. (2021). The first observation of N^+ electromagnetic ion cyclotron waves. *Journal of Geophysical Research: Space Physics*, *126*, e2020JA028716. https://doi.org/10.1029/2020JA028716

Received 30 SEP 2020
Accepted 26 DEC 2020

The First Observation of N^+ Electromagnetic Ion Cyclotron Waves

M. Fraz Bashir[1,2] and Raluca Ilie[2]

[1]Department of Earth, Planetary and Space Sciences, University of California Los Angeles, Los Angeles, CA, USA, [2]Department of Electrical and Computer Engineering, University of Illinois at Urbana-Champaign, Urbana, IL, USA

Abstract Observations from past space missions report on the significant abundance of N^+, in addition to those of O^+, outflowing from the terrestrial ionosphere and populating the near-Earth region. However, instruments on board current space missions lack the mass resolution to distinguish between the two, and often the role of N^+ in regulating the magnetosphere dynamics, is lumped together with that of O^+ ions. For instance, our understanding regarding the role of electromagnetic ion cyclotron (EMIC) waves in controlling the loss and acceleration of radiation belt electrons and ring current ions has been based on the contribution of He^+ and O^+ ions only. We report the first observations by Van Allen Probes of linearly polarized N^+ EMIC waves, which confirm the presence of N^+ in the terrestrial magnetosphere, and open up new avenues to particle energization, loss, and transport mechanisms, based on the altered magnetospheric plasma composition.

Plain Language Summary Electromagnetic ion cyclotron waves are believed to play an important role in regulating the dynamics of the Earth's magnetosphere. The presence of heavy ions even in small amounts significantly alters the propagation characteristics of EMIC waves. However, the mass spectrometers on-board the current magnetospheric missions are unable to reliably separate the N^+ from O^+. We report the first observation of N^+ EMIC waves, which have the potential to advance our understanding of the physical processes, which control the magnetospheric dynamics based on the relative contribution of N^+ and O^+.

1. Introduction

Electromagnetic ion cyclotron waves are predominately left-hand circularly polarized waves with small wave normal angle (WNA), and with frequencies below the proton cyclotron frequency (Horne & Thorne, 1993). EMIC waves are usually generated near the Earth's equator and tend to become more oblique and linearly polarized during their propagation toward higher latitudes. In the inner magnetosphere, EMIC waves are generated preferentially in regions where hot (~ 10–100 keV) ring current anisotropic ions and cold (~ few eVs) dense heavy ions spatially overlap (Cornwall, 1965; Jordanova et al., 2001; Kennel & Petschek, 1966). EMIC waves can also be generated in the dayside and nightside magnetosphere during times of enhanced solar wind dynamic pressure, which acts as a source of temperature anisotropy (Li et al., 2016; McCollough et al., 2012, 2010; Usanova et al., 2012). EMIC waves play a key role in the dynamic evolution of the Earth's magnetosphere, as they regulate the loss of ring current protons (Jordanova et al., 1996, 2006; Khazanov et al., 2006) and radiation belts electrons (Baker et al., 2004; Chen et al., 2010; Horne et al., 2005; Summers & Thorne, 2003; Usanova et al., 2014), heating of thermal electrons (Thorne et al., 2006; Zhou et al., 2013), and leading to an intensification of the proton aurora (Cornwall et al., 1970, 1971; Spasojevic et al., 2011; Yahnin et al., 2013).

The compositional changes in the magnetospheric plasma, such as the presence of heavy ions even in small amounts, alters the generation and propagation of EMIC waves, by reducing the phase speed and the instability threshold, enhancing the wave growth, and affecting the propagation away from the magnetic equator (Gary, 1993; Kozyra et al., 1984; Young et al., 1981). Therefore, the knowledge of the ion composition is essential to study their role in regulating the magnetospheric processes. In a multi-ion (H^+, He^+, O^+) plasma, we distinguish the multi-band structure separated by the heavy ion cyclotron frequency (Fraser & Nguyen, 2001; Jordanova et al., 2008; Chen et al., 2011, 2009; Usanova, Mann, & Darrouzet, 2016; Yu et al., 2018): H^+ band (between Ω_{H^+} and Ω_{He^+}), He^+ band (between Ω_{He^+} and Ω_{O^+}), and O^+ band be-

low Ω_{O^+}. However, observations from several past missions have clearly established the significant presence of N^+ ions, both in the ionosphere (Brinton et al., 1968; Craven et al., 1995; Hoffman, 1970; Hoffman et al., 1974; Ilie & Liemohn, 2016; Lin et al., 2020; Shelley et al., 1972; Taylor et al., 1968; Yau et al., 2009), and the magnetosphere (Chappell et al., 1982; Christon et al., 2002; Hamilton et al., 1988; Liu et al., 2005; Mall et al., 2002), and how their abundance changes as a function of solar cycle, season, and geomagnetic conditions. Nevertheless, most current space missions lack the possibility to reliably separate the N^+ from O^+ ions, owing to their very close masses, and the effect of N^+ in regulating the near-Earth plasma dynamics has not yet been quantified.

There are numerous studies that report the observations of EMIC waves based on the data obtained from Combined Release and Radiation Effects Satellite (Meredith et al., 2014, 2003), THEMIS (Min et al., 2012; Usanova et al., 2012), Van Allen probes (VAP) (Khazanov et al., 2017; Saikin et al., 2015; Wang et al., 2015; Yu et al., 2015), magnetospheric multiscale (MMS) (Wang et al., 2017), and Cluster (Allen et al., 2015, 2016) missions. A comprehensive statistical analysis of EMIC waves (H. Chen et al., 2019) based on Van Allen probes observations revealed that the H^+ band occurs at large L-shells ($5 \le L \le 6.5$) and in the noon sector ($9 \le \text{MLT} \le 16$), whereas He^+ (O^+) band is observed at low L-shells $3 \le L \le 4.5$ ($2 \le L \le 4$) in the morning (predawn) sector. H^+ and He^+ bands are left-handed polarized with moderate WNA (<40°) near the equator (magnetic latitude (MLAT) < 10°), and become linearly and oblique polarized as they propagate at larger MLATs, or large L-shells. The O^+ band is linearly polarized and has either small WNA (<20°) or large WNA (<50°). The free energy from the ring velocity distribution of ring current H^+ and O^+ ions, has been proposed as a possible generation mechanism for O^+ and He^+ EMIC waves occurring at low L-shells (Gamayunov et al., 2018; Usanova et al., 2018; Usanova, Mann, & Darrouzet, 2016; Yu et al., 2015, 2018). The source region of EMIC waves in the inner magnetosphere is confined within MLAT < 11°, but this is due to the observed bi-directional wave energy propagation both away and toward the equator (Loto'aniu et al., 2005; Usanova et al., 2013). However, there also exist off-equator source regions at high L-shells on the dayside, due to the formation of multiple magnetic field minima by solar wind compression (Usanova et al., 2008; Vines et al., 2019).

The presence of N^+ ions in the magnetospheric plasma alters the properties of EMIC waves and a new N^+ band (between Ω_{N^+} and Ω_{O^+}) is generated, which provides an additional resonant energy band that can promote scattering of relativistic electrons (Bashir & Ilie, 2018). In addition, it was shown that the N^+/O^+ ratio can vary from 0.6 to ~1 as the cutoff frequencies of hydrogen and helium increase. In this letter, we report the first observation of linearly polarized N^+ EMIC waves by the Van Allen Probes. We also discuss the possible generation mechanisms for the observed N^+ EMIC waves event based on the solar wind parameters, and storm time and local plasma conditions during this event.

2. Data Analysis

This study is based on the high-resolution data from the Electric and Magnetic Field Instrument Suite and Integrated Science (EMFISIS) (Kletzing et al., 2013) magnetometer instrument on-board the Van Allen Probes (Mauk et al., 2012). EMFISIS provides the wave properties, such as power spectral density (PSD), ellipticity, and wave normal angle (WNA). The magnetic field data, sampled at 64 Hz, is separated into the perturbed and average magnetic field through 100-s moving average in Geocentric Solar Magnetospheric (GSM) coordinates. The average magnetic field is used to calculate the ion cyclotron frequencies. To obtain the dynamic spectrogram of EMIC waves, the magnetic field is transformed from GSM coordinates into field-aligned coordinates, and then we applied the short-time Fast Fourier Transform with a sliding window of 100s, providing a frequency resolution of 0.01 Hz and a time resolution of about 14 s. We use the all three components of the perturbed magnetic field ($\delta B_{\perp 1}$, $\delta B_{\perp 2}$, $\delta B_{\parallel}$) to calculate the WNA and transverse components ($\delta B_{\perp 1}$ and $\delta B_{\perp 2}$) to calculate the ellipticity. The OMNI data set provided the solar wind parameters (density, velocity, interplanetary magnetic field), and geomagnetic activity (Sym-H, auroral electrojet (AE) and Kp indices). The Helium, Oxygen, Proton and Electron (HOPE) (Funsten et al., 2013) mass spectrometer measurements on-board Van Allen probes are used to extract density, temperatures, and temperature anisotropy values of hydrogen, helium, and oxygen ions.

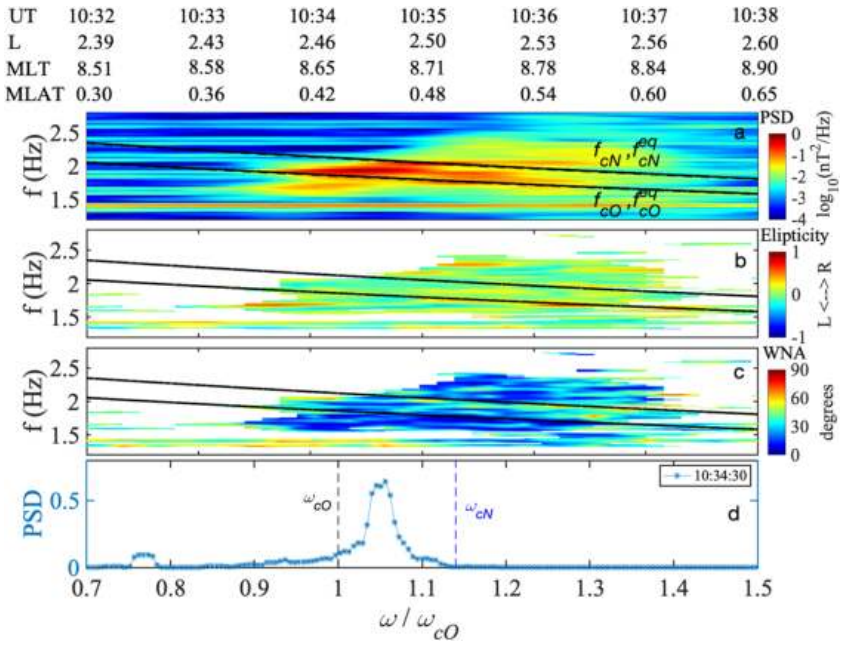

Figure 1. Wave properties of N^+ EMIC waves on September 8, 2017 as a function of Universal Time (UT), *L*-shell, magnetic local time (MLT), and magnetic latitude (MLAT): (a) power spectral density (PSD), (b), ellipticity, and **c**, wave normal angle (WNA) (0°–90°). The upper and lower black solid (dashed) curves show the local (equatorial) cyclotron frequency of nitrogen and oxygen respectively. Panels (a)–(c) show variations as function of UT, L, MLT and MLAT (upper *x*-axes). (d), The PSD as a function of normalized frequency (ω/ω_{co}) extracted at 10:34:30 UT.

3. First Observations of N^+ Electromagnetic Ion Cyclotron Waves

We report the first N^+ EMIC wave observation by the Van Allen probe A, based on data from the EMFISIS suite, on September 8, 2017, and as depicted in panel (a) of Figure 1. The N^+ EMIC wave of frequency (~ 1.8–2 Hz) is observed during the time interval (10:33:00–10:36:00), below the cyclotron frequency of nitrogen ions. The wave ellipticity (panel (b)) indicates that this N^+ EMIC wave is linearly polarized and it is propagating with a small WNA (≤30°). Note that the observed wave characteristics are similar to previous observations of O^+ EMIC waves. The local ($f_{c(N,O)}$) and the equatorial frequencies ($f^{eq}_{c(N,O)}$) overlap, and this is because the spacecraft is close to the equator (MLAT ~ 0.18–1.34°). The short duration of the event is possibly due to the fact the VAP-A is out-bounding at low *L*-shells (L ~ 2.45–2.55). Figure 1d shows the PSD as a function of frequency, extracted at the time of the first observed burst in wave activity (10:34:28 UT). The sharp peak between the oxygen and nitrogen cyclotron frequencies confirms the existence of a linearly polarized N^+ band EMIC waves.

Analysis of the solar wind parameters and geomagnetic conditions, in Figures 2a–2c, reveals that the N^+ EMIC wave is observed during the recovery phase of a geomagnetic storm, characterized by a minimum Sym-H of ~ −146 nT (panel (c)). The duration of the wave activity is denoted by the vertical dashed lines. The reduced part of Figure 2 is presented in Figure S1 which shows that the values of parameters are almost constant. The average constant values are shown by the arrow in Figure 2. The increase in solar wind dynamic pressure (McCollough et al., 2012) (panel (b)), and several subsequent injections (AE > 300) (Clausen et al., 2011), before the wave activity, could provide favorable conditions for the generation of N^+ EMIC waves.

Figures 3a–3c show the energy distribution of equatorially mirroring H^+ (panel (a)), He^+ (panel (b)), and the CNO^+ group ions (panel (c)). Note that the mass resolution of the HOPE instrument does not allow mass separation between N^+ and O^+ ions, and the observation of N^+ and the O^+ ions is considered here as the CNO^+ group. These measurements reveal that the hydrogen and helium ions are mostly warm (<100 eV), while the CNO^+ ions contribute to the energetic ring current population. During the time the wave activity is observed (denoted by the vertical dashed lines), the energy of CNO^+ ions significantly decreases, while

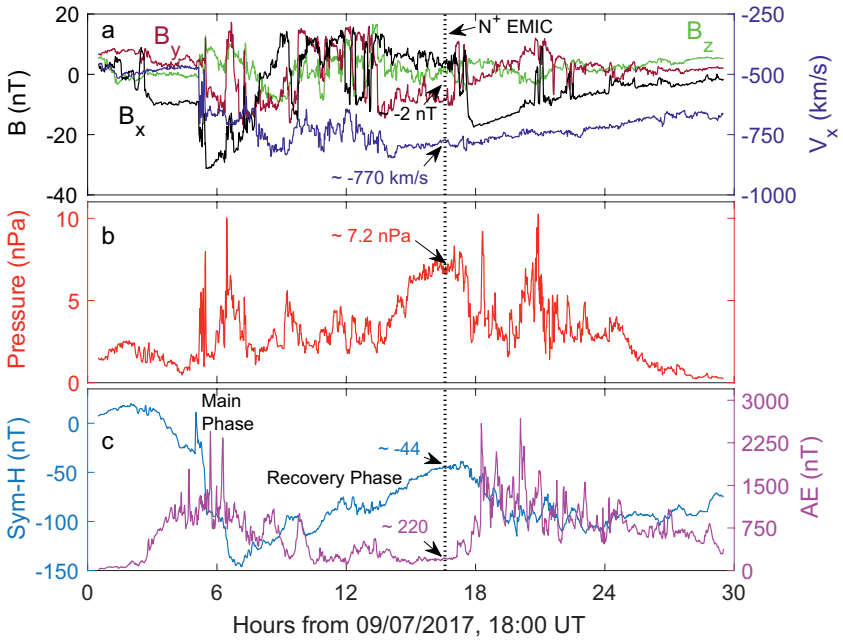

Figure 2. Solar wind conditions and geomagnetic indices from 18:00 UT of September 7, 2017. (a), The components of interplanetary magnetic field (IMF) B (nT), and the x-component of velocity v_x (km/s) in GSE coordinates on left and right axes, respectively, and (b) solar wind pressure (nPa). The Sym-H and AE indices are shown in (c). The region between two vertical black dotted lines represents the duration of N^+ EMIC waves activity (~10:33:00–10:36:00 UT). The approximate constant values of the parameters during the wave activity, are mentioned with arrows. The reduced part of Figure 2 showing constant values is given in Figure S1.

the protons get energized. Figures 3d–3g show the density (n_i), parallel ($T_\parallel$) and perpendicular ($T_\perp$) temperatures, and temperature anisotropy ($T_\perp/T_\parallel$) for H^+, He^+, and CNO^+ ions. The pitch angle dependent flux of CNO^+ ions (in Figure 3h) shows the butterfly distribution at lower ring current energies (<15 keV), whereas it becomes normal distribution for higher energy ions (~ 52 keV).

Instability analysis, based on the assumption that N^+ and O^+ have the same abundances (not shown here), does not support the hypothesis of a local generation mechanism of N^+ EMIC waves. This is due to the fact that proton density when the wave activity has been observed is relatively low, that is ~ 0.2 cm^{-3}, which is very small as compared to cold electron ~ 200 cm^{-3}, based on the electric field and wave density measurements. In addition, the proton temperature anisotropy $T_{h\perp}/T_{h\parallel} - 1 \sim 0.8$ and the parallel temperature $T_{h\parallel} = 1.2\ keV$ are lower than needed to indicate a local generation mechanism. However, possible dipolarization events and the associated particle injections, as denoted by the subsequent increases in the AE index (Figure 2, panel c) during the early recovery phase, could provide favorable conditions for the wave generation and propagation. It has been suggested that substorm injections can lead to EMIC wave generation if the injection occurs within 12 h of wave activity (Clausen et al., 2011). In the present case, intensification of the AE index is present within 10 h of generating N^+ EMIC waves.

Two possible scenarios can favor the generation of linearly polarized N^+ EMIC waves. One mechanism involves the presence of H^+ and/or O^+ ring velocity distributions (Gamayunov et al., 2018; Usanova et al., 2018; Usanova, Mann, & Darrouzet, 2016; Yu et al., 2015, 2018), which is different than the usual temperature anisotropy driven mechanism, and could explain the observations of these linearly polarized waves at low L-shells. The phase space distribution obtained from HOPE data (see Figure S2) depicts the presence of possible H^+ ring distribution around 0.5 and 1 keV. The other possibility is via the excitation due to mode conversion near the equatorial region (Kim et al, 2015, 2019; Lee et al., 2008; Miyoshi et al., 2019). Nevertheless, the existence of a linearly polarized N^+ band at low L-shells is in agreement with the previous observations of linearly polarized He^+ and O^+ bands (Gamayunov et al., 2018; Usanova, Malaspina, et al., 2016; Usanova et al., 2018; Yu et al., 2015). The wave power structure during the late recovery phase in the N^+ band can be relevant to the explanation given by (Paulson et al., 2017), and also the increase in the

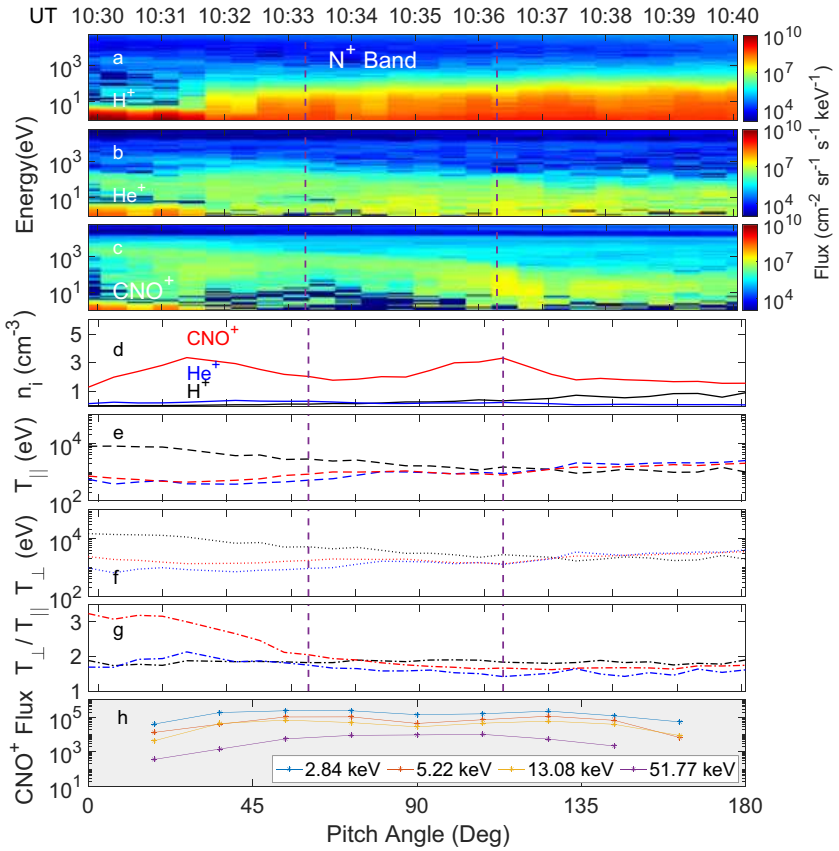

Figure 3. Energy distribution, plasma parameters, and pitch angle distribution from HOPE measurements by Van Allen probe A on September 8, 2017. (a–c) The energy distribution of hydrogen (H^+), helium (He^+), and CNO^+ ions, respectively. (d–g) The density, parallel and perpendicular temperatures and temperature anisotropy of proton (H^+), helium (He^+), and CNO^+ ions. Panels (a–g) show variations as a function of Universal Time (UT). (h) shows the CNO^+ flux as a function of pitch angle at time 10:35 and $L = 2.5$ for four different energies. The vertical dashed lines indicate the time period when the wave activity was observed. HOPE, Helium, Oxygen, Proton, and Electron.

radial extent of the resonance through dispersive effects is suggestive of a common source region as shown in the recent simulations (Kim et al., 2019). The generation mechanism of this N^+ EMIC wave event based on the possible sources discussed above needs further analysis and will be investigated in the future.

4. Summary of Results and Discussion

We report on the first observation of linearly polarized N^+ EMIC waves at low L-shells ($L < 4$), based on previously available measurements from instruments onboard the Van Allen Probes. The solar wind conditions reveal that the wave activity is observed during the recovery phase of 08 September 2017 storm, and the strong dayside compression and several subsequent particle injections associated with dipolarization events (AE > 300) could provide favorable conditions for the generation of the N^+ band. The wave activity is observed very close to the equator, and since the source region of EMIC wave in the inner magnetosphere seems to be confined within MLAT < 11° (Loto'aniu et al., 2005; Usanova et al., 2013), we speculate that the observed wave activity has its source near the equator.

The local plasma conditions do not favor a local generation mechanism. However, linearly polarized, small wave normal angles, N^+ EMIC waves observed at low L-shells can be generated via the mode conversion of compressional waves at the ion-ion hybrid/Buchsbaum resonance (Lee et al., 2008; Kim et al., 2015, 2019), and/or due to the free energy from ring velocity distribution of ring current protons (H^+) and oxygen (O^+) (Gamayunov et al., 2018; Usanova et al., 2018; Usanova, Mann, & Darrouzet, 2016; Yu et al., 2015, 2018).

However, this first observation of N^+ EMIC wave provides evidence of the N^+ ions presence in the near-Earth region, in addition to O^+, during this event. This study opens up the new avenues of quantifying the relative concentrations of N^+ and O^+ based on EMIC wave observations from current missions (e.g., Van Allen Probes, MMS, and Cluster), which can be used as a tool to infer the N^+ ion concentration using the observed characteristic frequencies (Kim et al., 2015; Min et al., 2015; Miyoshi et al., 2019). Inferred N^+ ion concentration can reveal N^+ torus and N^+ warm plasma cloak by quantifying O^+ torus (Nosé et al., 2018, 2020, 2015, 2011) and O^+ warm plasma cloak (Chappell et al., 2008). Also, the evidence of the existence of N^+ EMIC waves just above the oxygen cyclotron frequency, will help resolve the discrepancies of considering N^+ band as He^+ band, due to overlooking the N^+ existence. Quantifying the relative contribution of N^+ and O^+ to magnetospheric plasma, and distinguishing between N^+ and He^+ bands based on N^+ EMIC wave properties, have important implications for understanding the dynamics of the inner magnetosphere, as well as developing strategies to complement the current and future space missions.

Data Availability Statement

The Van Allen Probe data used in this study are available from https://spdf.gsfc.nasa.gov/pub/data/rbsp. The authors also acknowledge the use of OMNI data from CDAweb using https://cdaweb.sci.gsfc.nasa.gov.

Acknowledgments
M.F. Bashir is grateful to Lunjin Chen and Xiongdong Yu for insightful discussions. Research at UIUC was supported via AFOSR Young Investigator Research Program Award (AF FA9550-18-1-0195), NSF ICER Award 1664078 and NASA 80NSSC17K0015 (Sub MI 3004631577) and NASA ECIP 101049. The authors acknowledge the Van Allen Probes mission for the use of EMFISIS, HOPE, and EFW data in this study.

References

Allen, R. C., Zhang, J.-C., Kistler, L. M., Spence, H. E., Lin, R.-L., Klecker, B., et al. (2015). A statistical study of EMIC waves observed by Cluster: 1. Wave properties. *Journal of Geophysical Research: Space Phys.*, *120*, 5574–5592. https://doi.org/10.1002/2015JA021333

Allen, R. C., Zhang, J.-C., Kistler, L. M., Spence, H. E., Lin, R.-L., Klecker, B., et al. (2016). A statistical study of EMIC waves observed by Cluster: 2. Associated plasma conditions. *Journal of Geophysical Research: Space Physics*, *121*, 6458–6479. https://doi.org/10.1002/2016JA022541

Baker, D. N., Kanekal, S. G., Li, X., Monk, S. P., Goldstein, J., & Burch, J. L. (2004). An extreme distortion of the van allen belt arising from the Halloween solar storm in 2003. *Nature*, *432*(7019), 878–881. https://doi.org/10.1038/nature03116

Bashir, M. F., & Ilie, R. (2018). A new N^+ band of electromagnetic ion cyclotron waves in multi-ion cold plasmas. *Geophysical Research Letters*, *45*. 10150–10159. https://doi.org/10.1029/2018GL080280

Chappell, C. R., Huddleston, M. M., Moore, T. E., Giles, B. L., & Delcourt, D. C. (2008). Observations of the warm plasma cloak and an explanation of its formation in the magnetosphere. *Journal of Geophysical Research*, *113*(A9), A09206. https://doi.org/10.1029/2007JA012945

Chappell, C. R., Olsen, R. C., Green, J. L., Johnson, J. F. E., & Waite, J. H. W., Jr (1982). The discovery of nitrogen ions in the Earth's magnetosphere. *Geophysical Research Letters*, *9*, 937–940. https://doi.org/10.1029/GL009i009p00937

Chen, H., Gao, X., Lu, Q., & Wang, S. (2019). Analyzing EMIC waves in the inner magnetosphere using long-term Van Allen Probes observations. *Journal of Geophysical Research*, *124*, 7402–7412. https://doi.org/10.1029/2019JA026965

Chen, L., Thorne, R. M., & Bortnik, J. (2011). The controlling effect of ion temperature on EMIC wave excitation and scattering. *Geophysical Research Letters*, *38*, L16109. https://doi.org/10.1029/2011GL048653

Chen, L., Thorne, R. M., & Horne, R. B. (2009). Simulation of EMIC wave excitation in a model magnetosphere including structured high-density plumes. *Journal of Geophysical Research*, *114*, A07221. https://doi.org/10.1029/2009JA014204

Chen, L., Thorne, R. M., Jordanova, V. K., Wang, C., Gkioulidou, M., Lyons, L., & Horne, R. B. (2010). Global simulation of EMIC wave excitation during the 21 April 2001 storm from coupled RCM-RAM-HOTRAY modeling. *Journal of Geophysical Research*, *115*, A07209. https://doi.org/10.1029/2009JA015075

Christon, S. P., Mall, U., Eastman, T. E., Gloeckler, G., Lui, A. T. Y., McEntire, R. W., & Roelof, E. C. (2002). Solar cycle and geomagnetic N+1/O+1 variation in outer dayside magnetosphere: Possible relation to topside ionosphere. *Geophysical Research Letters*, *29*, 1058. https://doi.org/10.1029/2001GL013988

Clausen, L. B. N., Baker, J. B. H., Ruohoniemi, J. M., & Singer, H. J. (2011). EMIC waves observed at geosynchronous orbit during solar minimum: Statistics and excitation. *Journal of Geophysical Research*, *116*(A10), A10205. https://doi.org/10.1029/2011JA016823

Cornwall, J. M. (1965). Cyclotron instabilities and electromagnetic emission in the ultra low frequency and very low frequency ranges. *Journal of Geophysical Research*, *70*(1), 61–69. https://doi.org/10.1029/JZ070i001p00061

Cornwall, J. M., Coroniti, F. V., & Thorne, R. M. (1970). Turbulent loss of ring current protons. *Journal of Geophysical Research*, *75*, 4699. https://doi.org/10.1029/JA075i025p04699

Cornwall, J. M., Coroniti, F. V., & Thorne, R. M. (1971). Unified theory of SAR arc formation at the plasmapause. *Journal of Geophysical Research*, *76*, 4428. https://doi.org/10.1029/JA076i019p04428

Craven, P. D., Comfort, R. H., Richards, P. G., & Grebowsky, J. M. (1995). Comparisons of modeled N+, O+, H+, and He+ in the midlatitude ionosphere with mean densities and temperatures from atmosphere explorer. *Journal of Geophysical Research*, *100*(A1), 257–268.

Fraser, B. J., & Nguyen, T. S. (2001). Is the plasmapause a preferred source region of electromagnetic ion cyclotron waves in the magnetosphere? *Journal of Atmospheric and Solar-Terrestrial Physics*, *63*, 1225–1247. https://doi.org/10.1016/S1364-6826(00)00225-X

Funsten, H. O., Skoug, R. M., Guthrie, A. A., MacDonald, E. A., Baldonado, J. R., Harper, R. W., et al. (2013). Helium, oxygen, proton, and electron (hope) mass spectrometer for the radiation belt storm probes mission. *Space Science Reviews*, *179*(1), 423–484. https://doi.org/10.1007/s11214-013-9968-7

Gamayunov, K. V., Min, K., Saikin, A. A., & Rassoul, H. (2018). Generation of EMIC Waves observed by Van Allen Probes at low L shells. *Journal of Geophysical Research: Space Physics*, *123*(10), 8533–8556. https://doi.org/10.1029/2018JA025629

Gary, S. P. (1993). *Theory of space plasma microinstabilities*. Cambridge Atmospheric and Space Science Series, Cambridge, UK: Cambridge University Press. https://doi.org/10.1017/CBO9780511551512

Hamilton, D. C., Gloeckler, G., Ipavich, F. M., Wilken, B., & Stuede-mann, W. (1988). Ring current development during the great geomagnetic storm of February 1986. *Journal of Geophysical Research*, *93*, 14343–14355. https://doi.org/10.1029/JA093iA12p14343

Hoffman, J. H. (1970). Studies of the composition of the ionosphere with a magnetic deflection mass spectrometer. *International Journal of Mass Spectrometry and Ion Physics*, *4*, 315–322.

Hoffman, J. H., Dodson, W. H., Lippincott, C. R., & Hammack, H. D. (1974). Initial ion composition results from the Isis 2 satellite. *Journal of Geophysical Research*, *79*, 4246–4251.

Horne, R. B., & Thorne, R. M. (1993). On the preferred source location for the convective amplification of ion cyclotron waves. *Journal of Geophysical Research*, *98*(A6), 9233–9247. https://doi.org/10.1029/92JA02972

Horne, R. B., Thorne, R. M., Shprits, Y. Y., Meredith, N. P., Glauert, S. A., Smith, A. J., et al. (2005). Wave acceleration of electrons in the van allen radiation belts. *Nature*, *437*(7056), 227–230. https://doi.org/10.1038/nature03939

Ilie, R., & Liemohn, M. W. (2016). The outflow of ionospheric nitrogen ions: A possible tracer for the altitude- dependent transport and energization processes of ionospheric plasma. *Journal of Geophysical Research: Space Physics*, *121*, 9250–9255. https://doi.org/10.1002/2015JA022162

Jordanova, V. K., Albert, J., & Miyoshi, Y. (2008). Relativistic electron precipitation by EMIC waves from self-consistent global simulations. *Journal of Geophysical Research*, *113*, A00A10. https://doi.org/10.1029/2008JA013239

Jordanova, V. K., Farrugia, C. J., Thorne, R. M., Khazanov, G. V., Reeves, G. D., & Thomsen, M. F. (2001). Modeling ring current proton precipitation by electromagnetic ion cyclotron waves during the May 14–16, 1997, storm. *Journal of Geophysical Research*, *106*(A1), 7–22. https://doi.org/10.1029/2000JA002008

Jordanova, V. K., Kozyra, J. U., & Nagy, A. F. (1996). Effects of heavy ions on the quasi-linear diffusion coefficients from resonant interactions with electromagnetic ion cyclotron waves. *Journal of Geophysical Research*, *101*(A9), 19771–19778. https://doi.org/10.1029/96JA01641

Jordanova, V. K., Miyoshi, Y. S., Zaharia, S., Thomsen, M. F., Reeves, G. D., Evans, D. S., et al. (2006). Kinetic simulations of ring current evolution during the Geospace environment modeling challenge events. *Journal of Geophysical Research*, *111*, A11S10. https://doi.org/10.1029/2006JA011644

Kennel, C. F., & Petschek, H. E. (1966). Limit on stably trapped particle fluxes. *Journal of Geophysical Research*, *71*(1), 1–28. https://doi.org/10.1029/JZ071i001p00001

Khazanov, G. V., Boardsen, S., Krivorutsky, E. N., Engebretson, M. J., Sibeck, D., Chen, S., & Breneman, A. (2017). Lower hybrid frequency range waves generated by ion polarization drift due to electromagnetic ion cyclotron waves: Analysis of an event observed by the Van Allen Probe B. *Journal of Geophysical Research - A: Space Physics*, *122*, 449–463. https://doi.org/10.1002/2016JA022814

Khazanov, G. V., Gamayunov, K. V., Gallagher, D. L., & Kozyra, J. U. (2006). Self-consistent model of magnetospheric ring current and propagating electromagnetic ion cyclotron waves: Waves in multi-ion magnetosphere. *Journal of Geophysical Research*, *111*, A10202. https://doi.org/10.1029/2006JA011833

Kim, E.-H., Johnson, J. R., Kim, H., & Lee, D.-H. (2015). Inferring magnetospheric heavy ion density using emic waves. *Journal of Geophysical Research: Space Physics*, *120*(8), 6464–6473. https://doi.org/10.1002/2015JA021092

Kim, E.-H., Johnson, J. R., & Lee, D.-H. (2019). Electron inertial effects on linearly polarized electromagnetic ion cyclotron waves at Earth's magnetosphere. *Journal of Geophysical Research: Space Physics*, *124*(4), 2643–2655. https://doi.org/10.1029/2019JA026532

Kletzing, C. A., Kurth, W. S., Acuna, M., MacDowall, R. J., Torbert, R. B., Averkamp, T., et al. (2013). The electric and magnetic field instrument suite and integrated science (EMFISIS) on RBSP. *Space Science Reviews*, *179*, 127–181. http://dx.doi.org/10.1007/s11214-013-9993-6

Kozyra, J. U., Cravens, T. E., Nagy, A. F., Fontheim, E., & Ong, R. S. B. (1984). Effects of energetic heavy ions on electromagnetic ion cyclotron wave generation in the plasmapause region. *Journal of Geophysical Research*, *89*, 2217–2233. https://doi.org/10.1029/JA089iA04p02217

Lee, D.-H., Johnson, J. R., Kim, K., & Kim, K.-S. (2008). Effects of heavy ions on ULF wave resonances near the equatorial region. *Journal of Geophysical Research*, *113*(A11). https://doi.org/10.1029/2008JA013088

Li, L. Y., Yu, J., Cao, J. B., & Yuan, Z. G. (2016). Compression-amplified emic waves and their effects on relativistic electrons. *Physics of Plasmas*, *23*, 062116. https://doi.org/10.1063/1.4953899

Lin, M.-Y., Ilie, R., & Glocer, A. (2020). The contribution of N^+ ions to earth's polar wind. *Geophysical Research Letters*, *47*(18), e2020GL089321. https://doi.org/10.1029/2020GL089321

Liu, W. L., Fu, S. Y., Zong, Q.-G., Pu, Z. Y., Yang, J., & Ruan, P. (2005). Variations of N^+/O^+ in the ring current during magnetic storms. *Geophysical Research Letters*, *32*(15). https://doi.org/10.1029/2005GL023038

Loto'aniu, T. M., Fraser, B. J., & Waters, C. L. (2005). Propagation of electromagnetic ion cyclotron wave energy in the magnetosphere. *Journal of Geophysical Research*, *110*(A7), A07214. https://doi.org/10.1029/2004JA010816

Mall, U. A., Christon, S. P., Kirsch, E., & Gloeckler, G. (2002). On the solar cycle dependence of the N^+/O^+ content in the magnetosphere and its relation to atomic N and O in the Earth's exosphere. *Geophysical Research Letters*, *29*, 1593. https://doi.org/10.1029/2001GL013957

Mauk, B. H., Fox, N. J., Kanekal, S. G., Kessel, R. L., Sibeck, D. G., & Ukhorskiy, A. (2012). Science objectives and rationale for the radiation belt storm probes mission. *Space Science Reviews*, *179*, 3–27. http://dx.doi.org/10.1007/s11214-012-9908-y

McCollough, J. P., Elkington, S. R., & Baker, D. N. (2012). The role of Shabansky orbits in compression-related electromagnetic ion cyclotron wave growth. *Journal of Geophysical Research*, *117*, A01208. https://doi.org/10.1029/2011JA016948

McCollough, J. P., Elkington, S. R., Usanova, M. E., Mann, I. R., Baker, D. N., & Kale, Z. C. (2010). Physical mechanisms of compressional emic wave growth. *Journal of Geophysical Research*, *115*(A10). https://doi.org/10.1029/2010JA015393

Meredith, N. P., Horne, R. B., Kersten, T., Fraser, B. J., & Grew, R. S. (2014). Global morphology and spectral properties of EMIC wavesderived from CRRES observations. *Journal of Geophysical Research - A: Space Physics*, *119*, 5328–5342. https://doi.org/10.1002/2014JA020064

Meredith, N. P., Thorne, R. M., Horne, R. B., Summers, D., Fraser, B. J., & Anderson, R. R. (2003). Statistical analysis of relativistic electron energies for cyclotron resonance with EMIC waves observed on CRRES. *Journal of Geophysical Research*, *108*, 1250. https://doi.org/10.1029/2002JA009700

Min, K., Lee, J., Keika, K., & Li, W. (2012). Global distribution of EMIC waves derived from THEMIS observations. *Journal of Geophysical Research*, *117*, A05219. https://doi.org/10.1029/2012JA017515

Min, K., Liu, K., Bonnell, J. W., Breneman, A. W., Denton, R. E., Funsten, H. O., et al. (2015). Study of EMIC wave excitation using direct ion measurements. *Journal of Geophysical Research: Space Physics*, *120*, 2702–2719. https://doi.org/10.1002/2014JA020717

Miyoshi, Y., Matsuda, S., Kurita, S., Nomura, K., Keika, K., Shoji, M., et al. (2019). Emic waves converted from equatorial noise due to m/q = 2 ions in the plasmasphere: Observations from van allen probes and Arase. *Geophysical Research Letters*, *46*(11), 5662–5669. https://doi.org/10.1029/2019GL083024

Nosé, M., Matsuoka, A., Kumamoto, A., Kasahara, Y., Goldstein, J., Teramoto, M., et al. (2018). Longitudinal structure of oxygen torus in the inner magnetosphere: Simultaneous observations by arase and van Allen probe a. *Geophysical Research Letters*, *45*(19). 10177–10184. https://doi.org/10.1029/2018GL080122

Nosé, M., Matsuoka, A., Kumamoto, A., Kasahara, Y., Teramoto, M., Kurita, S., et al. (2020). Oxygen torus and its coincidence with emic wave in the deep inner magnetosphere: Van allen probe b and arase observations. *Earth Planets and Space*, *72*(1), 111. https://doi.org/10.1186/s40623-020-01235-w

Nosé, M., Oimatsu, S., Keika, K., Kletzing, C. A., Kurth, W. S., Pascuale, S. D., et al. (2015). Formation of the oxygen torus in the inner magnetosphere: Van allen probes observations. *Journal of Geophysical Research: Space Physics*, *120*(2), 1182–1196. https://doi.org/10.1002/2014JA020593

Nosé, M., Takahashi, K., Anderson, R. R., & Singer, H. J. (2011). Oxygen torus in the deep inner magnetosphere and its contribution to recurrent process of O+-rich ring current formation. *Journal of Geophysical Research*, *116*(A10), A10224. https://doi.org/10.1029/2011JA016651

Paulson, K. W., Smith, C. W., Lessard, M. R., Torbert, R. B., Kletzing, C. A., & Wygant, J. R. (2017). In situ statistical observations of pc1 pearl pulsations and unstructured emic waves by the van allen probes. *Journal of Geophysical Research: Space Physics*, *122*(1), 105–119. https://doi.org/10.1002/2016JA023160

Saikin, A. A., Zhang, J.-C., Allen, R. C., Smith, C. W., Kistler, L. M., Spence, H. E., et al. (2015). The occurrence and wave properties of H^+−, He^+−, and O^+−band EMIC waves observed by the Van Allen Probes. *Journal of Geophysical Research: Space Physics*, *120*, 7477–7492. https://doi.org/10.1002/2015JA021358

Shelley, E. G., Johnson, R. G., & Sharp, R. D. (1972). Satellite observations of energetic heavy ions during a geomagnetic storm. *Journal of Geophysical Research*, *77*, 6104. https://doi.org/10.1029/JA077i031p06104

Spasojevic, M., Blum, L. W., MacDonald, E. A., Fuselier, S. A., & Golden, D. I. (2011). Correspondence between a plasma-based EMIC wave proxy and subauroral proton precipitation. *Geophysical Research Letters*, *38*, L23102. https://doi.org/10.1029/2011GL049735

Summers, D., & Thorne, R. M. (2003). Relativistic electron pitch-angle scattering by electromagnetic ion cyclotron waves during geomagnetic storms. *Journal of Geophysical Research*, *108*, 1143. https://doi.org/10.1029/2002JA009489

Taylor, H. A., Brinton, H. C., Pharo, M. W., & Rahman, N. K. (1968). Thermal ions in the exosphere; Evidence of solar and geomagnetic control. *Journal of Geophysical Research*, *73*(17), 5521–5533. https://doi.org/10.1029/ja073i017p05521

Taylor, H. A. J., Brinton, H. C., Pharo, M. W. I., & Rahman, N. K. (1968). Thermal ions in the exosphere; Evidence of solar and geomagnetic control. *Journal of Geophysical Research*, *73*(1), 5521–5533.

Thorne, R. M., Horne, R. B., Jordanova, V. K., Bortnik, J., & Glauert, S. (2006). Interaction of EMIC waves with thermal plasma and radiation belt particles, In K. Takahashi, P. J. Chi, R. E. Denton, R. L. Lysak. (Eds.), *Magnetospheric ULF waves: Synthesis and new directions, Geophysical Monograph Series* (Vol. *169*). AGU.

Usanova, M. E., Ahmadi, N., Malaspina, D. M., Ergun, R. E., Trattner, K. J., Reece, Q., et al. (2018). MMS observations of harmonic electromagnetic ion cyclotron waves. *Geophysical Research Letters*, *45*(17), 8764–8772. https://doi.org/10.1029/2018GL079006

Usanova, M. E., Darrouzet, F., Mann, I. R., & Bortnik, J. (2013). Statistical analysis of emic waves in plasmaspheric plumes from cluster observations. *Journal of Geophysical Research: Space Physics*, *118*(8), 4946–4951. https://doi.org/10.1002/jgra.50464

Usanova, M. E., Drozdov, A., Orlova, K., Mann, I. R., Shprits, Y., Robertson, M. T., et al. (2014). Effect of EMIC waves on relativistic and ultra-relativistic electron populations: Ground-based and Van Allen Probes observations. *Geophysical Research Letters*, *41*, 1375–1381. https://doi.org/10.1002/2013GL059024

Usanova, M. E., Malaspina, D. M., Jaynes, A. N., Bruder, R. J., Mann, I. R., Wygant, J. R., & Ergun, R. E. (2016). Van allen probes observations of oxygen cyclotron harmonic waves in the inner magnetosphere. *Geophysical Research Letters*, *43*(17), 8827–8834. https://doi.org/10.1002/2016GL070233

Usanova, M. E., Mann, I. R., Bortnik, J., Shao, L., & Angelopoulos, V. (2012). THEMIS observations of electromagnetic ion cyclotron wave occurrence: Dependence on AE, SYMH, and solar wind dynamic pressure. *Journal of Geophysical Research*, *117*, A10218. https://doi.org/10.1029/2012JA018049

Usanova, M. E., Mann, I. R., & Darrouzet, F. (2016). EMIC waves in the inner magnetosphere. In A. Keiling, D. Lee, & V. Nakariakov (Eds.), *Low frequency waves in space plasmas*. John Wiley and Sons. https://doi.org/10.1002/9781119055006.ch5

Usanova, M. E., Mann, I. R., Rae, I. J., Kale, Z. C., Angelopoulos, V., Bonnell, J. W., et al. (2008). Multipoint observations of magnetospheric compression-related EMIC Pc1 waves by THEMIS and CARISMA. *Geophysical Research Letters*, *35*(17). https://doi.org/10.1029/2008GL034458

Vines, S. K., Allen, R. C., Anderson, B. J., Engebretson, M. J., Fuselier, S. A., Russell, C. T., et al. (2019). EMIC waves in the outer magnetosphere: Observations of an off-equator source region. *Geophysical Research Letters*, *46*(11), 5707–5716. https://doi.org/10.1029/2019GL082152

Wang, D., Yuan, Z., Yu, X., Deng, X., Zhou, M., Huang, S., et al. (2015). Statistical characteristics of EMIC waves: Van Allen Probe observations. *Journal of Geophysical Research: Space Physics*, *120*, 4400–4408. https://doi.org/10.1002/2015JA021089

Wang, X. Y., Huang, S. Y., Allen, R. C., Fu, H. S., Deng, X. H., Zhou, M., et al. (2017). The occurrence and wave properties of EMIC waves observed by the Magnetospheric Multiscale (MMS) mission. *Journal of Geophysical Research: Space Physics*, *122*, 8228–8240. https://doi.org/10.1002/2017JA024237

Yahnin, T. A., Yahnina, A. G., Frey, H., & Pierrard, V. (2013). Sub-oval proton aurora spots: Mapping relatively to the plasmapause. *Journal of Atmospheric and Solar-Terrestrial Physics*, *99*, 61–66. https://doi.org/10.1016/j.jastp.2012.09.018

Yau, A., James, H. G., Bernhardt, P. A., Cogger, L. L., Enno, G. A., Hayakawa, H., et al. (2009). The Canadian enhanced polar outflow probe (e-POP) mission. *Data Science Journal*, *8*(0), S38–S44.

Young, D. T., Perraut, S., Roux, A., de Villedary, C., Gendrin, R., Korth, A., et al. (1981). Wave-particle interactions near Ω_{He+} observed on GEOS 1 and 2 1. Propagation of ion cyclotron waves in He^+-rich plasma. *Journal of Geophysical Research*, *86*(A8), 6755–6772. https://doi.org/10.1029/JA086iA08p06755

Yu, X., Yuan, Z., Huang, S., Yao, F., Wang, D., Funsten, H. O., & Wygant, J. R. (2018). Excitation of O+ band EMIC waves through H+ ring velocity distributions: Van Allen Probe observations. *Geophysical Research Letters*, *45*(3), 1271–1276. https://doi.org/10.1002/2018GL077109

Yu, X., Yuan, Z., Wang, D., Li, H., Huang, S., Wang, Z., et al. (2015). In situ observations of EMIC waves in O^+ band by the Van Allen Probe A. *Geophysical Research Letters*, *42*, 1312–1317. https://doi.org/10.1002/2015GL063250

Zhou, Q., Xiao, F., Yang, C., He, Y., & Tang, L. (2013). Observation and modeling of magnetospheric cold electron heating by electromagnetic ion cyclotron waves. *Journal of Geophysical Research: Space Physics*, *118*, 6907–6914. https://doi.org/10.1002/2013JA019263